



Effect of Eu doping on the structure, morphology and luminescence properties of ZnO submicron rod for white LED applications

Mei Xin^{1,2}

Received: 3 April 2018 / Accepted: 10 October 2018 / Published online: 17 October 2018
© The Author(s) 2018

Abstract

Eu³⁺-doped ZnO submicron rod has been prepared by a hydrothermal method. Synthesized rods are characterized by X-ray diffraction, scanning electron microscopy and photoluminescence spectra (PL). The results indicated structures and morphology of rods affected by the Eu³⁺ doping concentration. ⁵D_{0–7}F_J (*J* = 1, 2 and 3) of Eu³⁺ emission appeared, and energy transfer from the ZnO host and deep defects of ZnO to Eu³⁺ in the ZnO:Eu is occurred. Strong and white emission was observed in the sample with 15% Eu.

Keywords Eu-doped ZnO · Hydrothermal method · Submicron rod · White-light emission

Introduction

Today, the clean and renewable energy sources are very important because of limitations of fossil fuel and environmental problems. Semiconductor materials with different structures and morphology are used in various research and development fields of clean and renewable energy due to their unique characteristics [1–3]. The structure, morphology and properties of semiconductor materials are bound not only to precursor materials and preparation methods, but also to dopants and annealing temperatures [4–6]. Among the semiconductor materials, ZnO with a wide band gap (3.37 eV) is an II–VI semiconductor and it has a large exciton binding energy of 60 meV [7–10]. ZnO exhibits excellent physical and chemical properties which make it a unique host material for numerous devices by doping with different rare earth ions. Rare earth (RE) doping of ZnO can expand its optical and electronic properties because of their narrow and intense emission lines due to intra-4*f* transitions [11, 12]. Among them, the Eu³⁺-doped ZnO (ZnO:Eu) raised a lot of interest because of the red emission from the Eu³⁺

[13]. As a new energy source in the field of lighting, ZnO doped with rare earth ions is utilized for advanced full-color display and white LEDs lighting applications. For fabrication of white-light emitters, *n*-UV (370–410 nm) LEDs are usually combined with red/green/blue tricolor phosphors [14, 15]. However, using two or three different phases of phosphors leads to decrease luminous efficiency. A single full-color emitting phosphor for *n*-UV LED is under an obligation to enhance luminous efficiency and reproducibility of white LED [16, 17]. Pure ZnO generally emits blue–green light, because of its inherent defects. Furthermore, bright red emission from Eu³⁺ is expected and this needs the efficient energy transfer between the ZnO matrixes to Eu³⁺ emission centers. However, due to the considerable difference of chemical properties between Eu³⁺ (0.98 Å) and Zn²⁺ (0.77 Å), it is hard to substitute Eu³⁺ ions for Zn²⁺ ions in ZnO [18]. The emissions of Eu³⁺ ions are sensitive to the local environment or symmetry of the host materials [19]. In recent years, many researchers indicate that Eu³⁺ ions can incorporate into the ZnO matrix under suitable conditions because they observe the efficient red emissions from Eu³⁺-doped ZnO [11]. Therefore, several preparation techniques have been used to synthesize the Eu-doped ZnO such as sol–gel [20], microwave-assisted combustion [21], solid-state reaction [22], magnetron sputtering [23], hydrothermal [19, 24, 25], chemical vapor deposition [26, 27] and electrodeposition [28]. Particularly, the hydrothermal method is considered as an attractive preparation process of Eu-doped ZnO due to the simplicity, low cost, the possibility of mass

✉ Mei Xin
xinmei_dl@126.com

¹ School of Physics and Materials Engineering, Dalian Nationalities University, Dalian 116600, China

² Liaoning Key Laboratory of Optoelectronic Films and Materials, Dalian Nationalities University, Dalian 116600, China

production and the environmental friendliness. However, there are few reports of ZnO:Eu as a white powder. In this paper, Eu-doped ZnO is synthesized using hydrothermal method. Detailed investigations of Eu doping on morphological and crystalline structures of synthesized ZnO and PL properties and the energy transfer mechanism are discussed.

Experimental

Material preparations

ZnO:Eu³⁺ was synthesized using hydrothermal method. All reactants were of reagent grade. ZnO doped with different Eu³⁺ concentrations was synthesized. In a typical experiment, 35 mL of 0.05 M zinc acetate (Zn(CH₃COO)₂·2H₂O) was dissolved in distilled water, and 2.1 mL of 13.3 M ammonia (NH₃), 5.25 mL of 0.05 M Eu(NO₃)₃·6H₂O were mixed under magnetic stirring. The molar ratio of Eu/Zn is 0.05(5%), 0.10(10%), 0.15 (15%) and 0.20(20%) in the mixed solution, respectively. The resulting precipitate was enclosed in a Teflon-lined autoclave with 50 mL capacity. The closed autoclave was placed into the furnace at a preset temperature of 200 °C for 12 h and then cooled to room temperature naturally. The resulting precipitate was filtered off and washed 1 time in distilled water. The final product was dried in air at 60 °C for 12 h.

Materials characterization

Crystal structures of the ZnO:Eu were analyzed by using an X-ray diffraction (XRD) (XRD-6000, Shimadzu Corporation). The morphology of the samples was characterized using scanning electron microscopy (SEM) (Hitachi S4800 SEM). Photoluminescence (PL) measurements were taken by HITACHI F-4600 spectrophotometer.

Results and discussion

Morphology and structure analysis

Figure 1 shows SEM images of the undoped, 5% and 15% Eu-doped ZnO materials synthesized by a hydrothermal method. It can become quite clear that undoped ZnO in Fig. 1a shows submicron rod and their diameter is about 200 nm (insert of Fig. 1a). The rod's end looks just like a taper. For ZnO doped with 5% Eu and 15%, shown in Fig. 1b, c, the diameter is about 300 nm (insert of Fig. 1b) and 600 nm (insert of Fig. 1c), respectively, and they have flat facets at both ends. From above results both crystallite size and their crystal growth are influenced significantly by Eu doping. The chemical potential of a crystal plane is

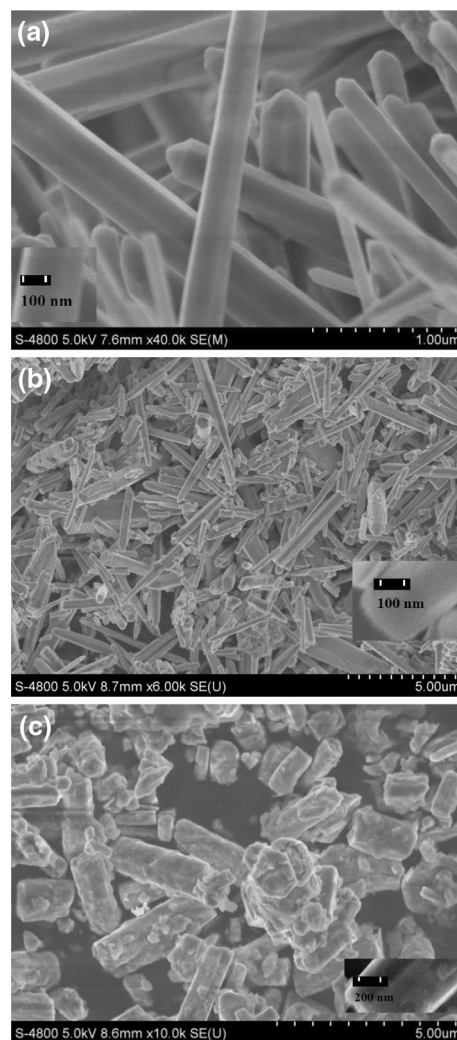


Fig. 1 SEM images of ZnO:Eu submicrorods **a** undoped ZnO; **b** 5%; **c** 15% Eu-doped sample

determined by the average number of dangling bonds per atom over the entire crystal facet [29]. The different density of Eu³⁺ on various crystal planes leads to the difference in chemical potential of crystal facets. The different chemical potential of crystal facets has different growth rates. The growth rate along the diameter is much quicker than that along the top side, which may lead the rod diameter to increase with Eu doping.

Figure 2 shows XRD patterns of ZnO:Eu³⁺ with different concentrations of Eu³⁺. It is clear that all of the XRD peaks of the samples match with the values of the standard card for zincite ZnO (JCPDS No. 36-1451). In total, 20% Eu-doped samples detected a weak impurity peak observed at 29.4 (marked with an asterisk) is assigned to Eu₂O₃ (JCPDS No. 43-1009) [13]. ZnO peak intensity increases with increasing the doping concentrations from 0 to 5% and decreases with increasing the doping

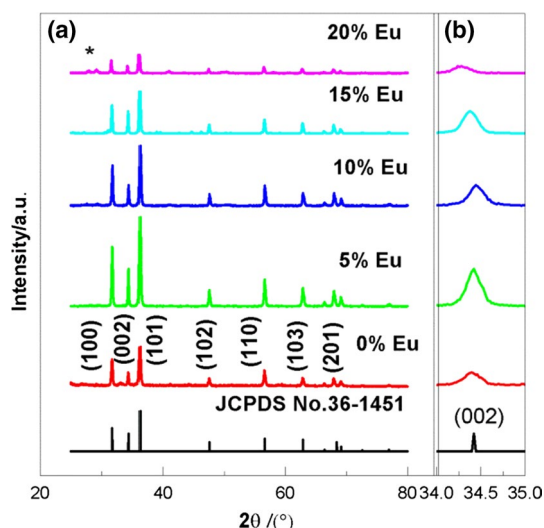


Fig. 2 XRD patterns of **a** undoped and different Eu-doped ZnO submicrorods and **b** (002) peak positions of undoped and different Eu-doped ZnO submicrorods

concentrations from 10 to 20%. Comparing the XRD patterns of undoped and different Eu-doped ZnO, a slight shift to higher angles of peak positions is observed with increasing Eu concentration to 10% and a slight shift to lower angles of peak positions is observed with further increasing the Eu content. [Figure 2 shows the shift of (002) peak positions.] The common defects in ZnO such as oxygen, zinc vacancies and oxygen interstitials are produced in preparing process. The incorporation of Eu may lead to the formation of four kinds of configuration in ZnO's host lattice for $\text{ZnO}:\text{Eu}_{\text{Zn}}$, $\text{ZnO}:\text{Eu}_{\text{I}}$, $\text{ZnO}:\text{Eu}_{\text{Zn}} + \text{V}_{\text{O}}$ and $\text{ZnO}:\text{Eu}_{\text{Zn}} + \text{Zn}_{\text{I}}$, respectively [30, 31]. Considering structural stability with less lattice distortion, the substitutional Eu an oxygen interstitial to form $(\text{Eu}_{\text{Zn}} + \text{O}_{\text{I}})$ complexes [30, 31]. The XRD peak position of (002) moves to a slight higher angle as compared to that of ZnO, indicating that the lattice parameter is decreased after doping of Eu. A decrease in the lattice parameters is rather a sign of the formation of defect complexes [32]. Therefore, it shows that the $\text{Eu}_{\text{Zn}} + \text{O}_{\text{I}}$ complexes are formed and dominant at the doping concentration which is less than 10%. The XRD (002) peak position of 15–20% samples moves to a slightly lower scattering angle. It indicated that a small amount of Eu^{3+} ions has been successfully doped into the crystal lattice of ZnO host to form Eu_{Zn} . The larger Eu^{3+} substituted the Zn^{2+} and results in the expansion of the unit-cell volume of the Eu-doped samples [16]. The intensity of the (002) diffraction peak increases with the Eu molar ratio until 5% and then decreases, at further increase in Eu doping.

PL properties

Figure 3 displays the PL excitation (PLE) spectra of the 15% Eu-doped ZnO rods. In the PLE, the monitoring emission was set at 618 nm, the observed peaks are centered at 380 nm belonging to ZnO, and 394 and 464 nm are ascribed to the direct excitation of the Eu^{3+} ions from the ground state (${}^7\text{F}_0$) to different excited levels (${}^5\text{L}_6$, ${}^5\text{D}_2$) [20], and 532 nm is related to deep defects of ZnO, respectively. The strongest excitation peak is located at 394 nm. Figure 4 shows the PL spectra of Eu-doped ZnO submicron rods under the excitation of 394 nm. Series of characteristic Eu^{3+} ion emissions centered at 593, 618 and 652 nm are, respectively, attributed to intra-4f transitions of ${}^5\text{D}_0 \rightarrow {}^7\text{F}_1$, ${}^5\text{D}_0 \rightarrow {}^7\text{F}_2$, ${}^5\text{D}_0 \rightarrow {}^7\text{F}_3$ of Eu^{3+} ions. The most prominent emissions are set at 593 nm and 618 nm. The peak set at 593-nm emission attributed to ${}^5\text{D}_0 \rightarrow {}^7\text{F}_1$

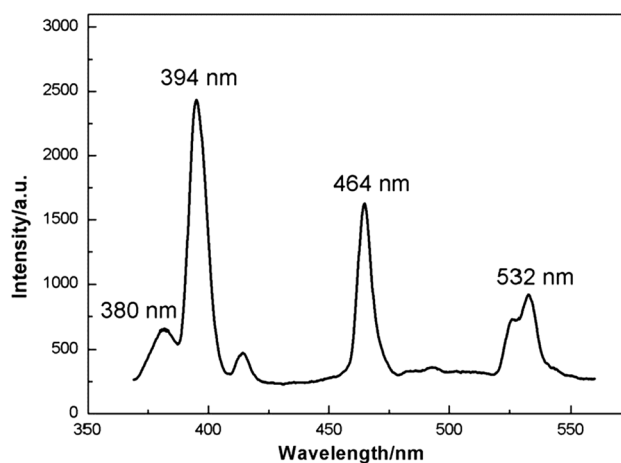


Fig. 3 PLE spectrum of 15% Eu-doped ZnO microrod monitored at 618 nm

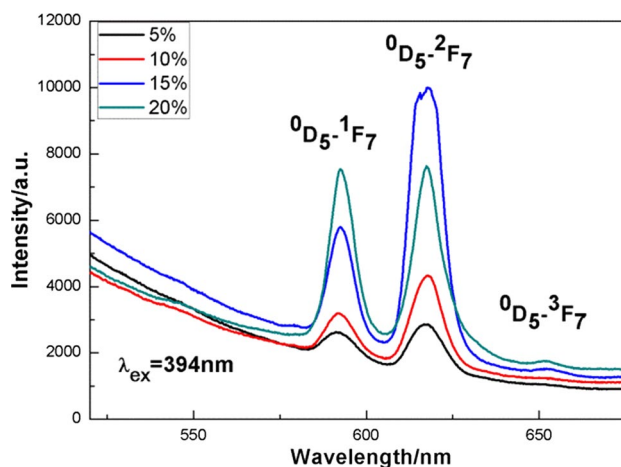


Fig. 4 PL spectra of different Eu-doped ZnO samples under excitation of 394 nm

transition is a magnetic dipole transition, which is not affected by the crystal environment of the host materials. The strongest emission peak is at 618 nm, attributed to ${}^5D_0 \rightarrow {}^7F_2$ transition, which is a hypersensitive forced electric-dipole transition and the ${}^5D_0 \rightarrow {}^7F_2$ transition with $\Delta J = 2$ is a forbidden transition in the free ion. It is noted only when the Eu^{3+} ions are in a low symmetry position and no inversion center [10, 18]. The red emission intensity was increasing in increasing the Eu^{3+} concentration. The strongest ${}^5D_0 \rightarrow {}^7F_2$ emission intensity of ZnO:Eu comes from the 15% Eu doping sample. To 20% Eu doping sample, the emission intensity decreased owing to concentration quenching. The transition of ${}^5D_0 \rightarrow {}^7F_1$ is independent of the host lattice and therefore of the intensity ratio of red to orange emission. S increases with decreasing lattice symmetry, such as formula (1) [33]

$$S_{\text{Eu}^{3+}} = \int (I)_{618 \text{ nm}} d\lambda / \int (I)_{593 \text{ nm}} d\lambda \quad (1)$$

The calculated $S_{\text{Eu}^{3+}}$ of different concentrations of Eu doping samples is as shown in Fig. 5. The value of $S_{\text{Eu}^{3+}}$ is a maximum of 3.02 at 15% doping, and the $S_{\text{Eu}^{3+}}$ value decreases as the doping concentration increases further. This is indicated that for 15% doping concentration more Eu^{3+} ions are located in a low symmetry position.

Figure 6 shows the PL spectra of undoped and 15% Eu-doped ZnO samples under excitation of 394 nm. The broad blue–green emission around 455 nm is observed in the undoped sample. It is from the structural defects of ZnO host such as oxygen and zinc interstitials. After doping with Eu, the strongest Eu^{3+} -related emission is observed and the blue–green emission intensity decreased. The Eu^{3+} -related emission can also be observed under 380- and 532-nm excitation (see Fig. 7). The result indicated

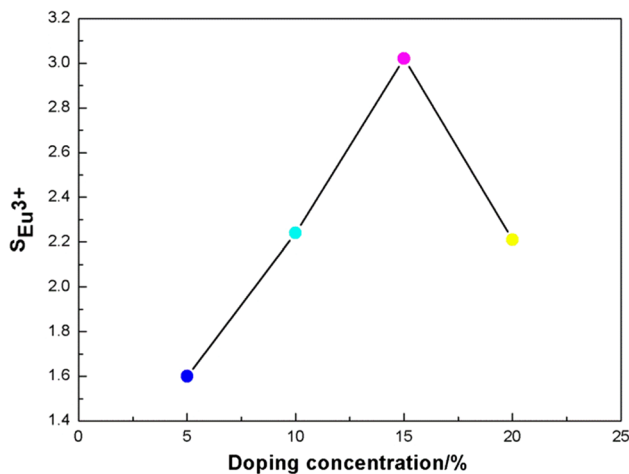


Fig. 5 The calculated $S_{\text{Eu}^{3+}}$ of 5%, 10%, 15% and 20% Eu-doped ZnO samples under excitation of 394 nm

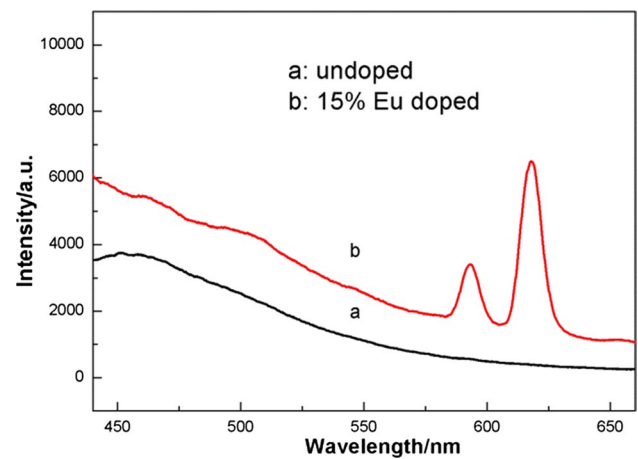


Fig. 6 PL spectra of undoped and 15% Eu-doped ZnO samples under excitation of 394 nm

that energy transfer from ZnO and deep defects of ZnO to Eu^{3+} has appeared.

Figure 8 shows the chromaticity coordinate of 15% Eu doping sample excited by 394 nm and shown on the CIE 1931 color diagram. The color coordinates of (0.25872, 0.26152) in 15% Eu doping ZnO are found to be set in the standard white-light oval, and the white light is achieved by the superposition of the blue–green emission from defects of ZnO and the red emission from Eu^{3+} ions, which reveals that ZnO:Eu is a potential candidate for fabricating near (*n*)-ultraviolet (UV) or blue-converted LEDs white-light-emitting materials.

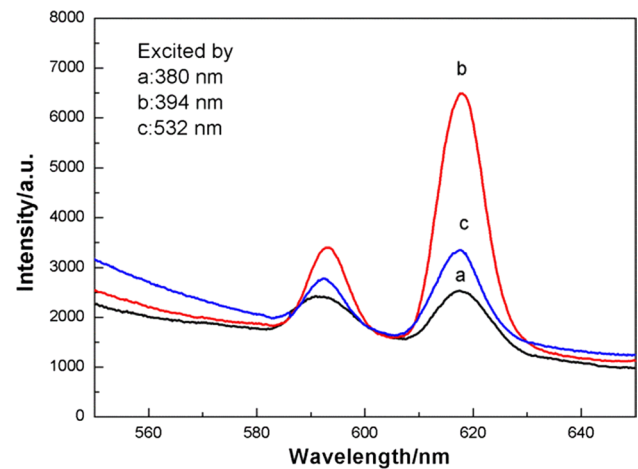


Fig. 7 PL spectra of 15% Eu-doped ZnO excited by different wavelength

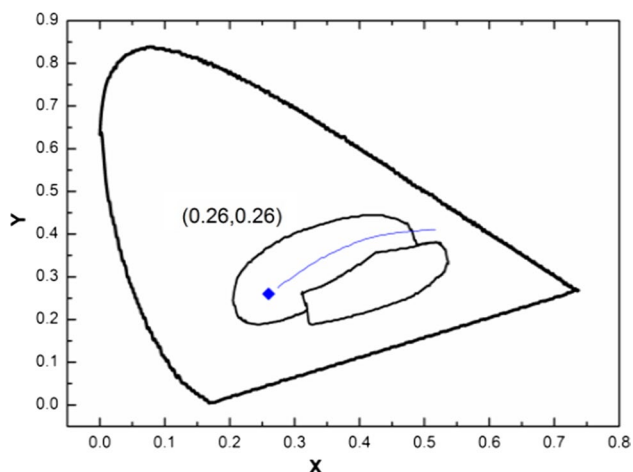


Fig. 8 CIE-1931 chromaticity coordinates of 15 at.% Eu doping ZnO ($\lambda_{exc} = 394$ nm)

Conclusions

We have synthesized the ZnO:Eu submicron rods by a simple hydrothermal method. SEM and XRD studies reveal that the rod's diameter increases with the increase in the Eu concentration. The XRD peak positions gradually shifted toward higher scattering angle firstly and then shifted toward lower diffraction angle with increasing Eu doping. The Eu^{3+} -related emissions appeared in Eu doping samples. The strongest red emission was obtained from 15% Eu^{3+} doping; the sample due to the energy transfer from ZnO and deep defects of ZnO to Eu^{3+} has appeared. The color coordinate (x, y) of 15% Eu doping phosphor is (0.2587, 0.2615) which is located on the standard white-light oval under the excitation at 394 nm. Doping forms of Eu are discussed. The results would be helpful for ZnO:Eu in optoelectronic device applications.

Acknowledgement This work was supported by a Doctoral Fund of Dalian Nationalities University (20116201), Independent Fund Project of Central University (110207).

Open Access This article is distributed under the terms of the Creative Commons Attribution 4.0 International License (<http://creativecommons.org/licenses/by/4.0/>), which permits unrestricted use, distribution, and reproduction in any medium, provided you give appropriate credit to the original author(s) and the source, provide a link to the Creative Commons license, and indicate if changes were made.

References

- Naseri, N., Soleymani, S., Ghaderi, A., Bramowicz, M., Kulesza, S., Țălu, Ș., Pourreza, M., Ghasemi, S.: Microstructure, morphology and electrochemical properties of Co nanoflake water oxidation electrocatalyst at micro- and nanoscale. *RSC Adv.* **7**(21), 12923–12930 (2017). <https://doi.org/10.1039/c6ra28795f>
- Țălu, Ș., Bramowicz, M., Kulesza, S., Ghaderi, A., Soleymani, S., Savaloni, H., Babaei, R.: Micromorphology analysis of specific 3-D surface texture of silver chiral nanoflower sculptured structures. *J. Ind. Eng. Chem.* **43**, 164–169 (2016). <https://doi.org/10.1016/j.jiec.2016.08.003>
- Zare, M., Soleymani, S., Shafiekhani, A., Kulesza, S., Talu, S., Bramowicz, M.: Evolution of rough-surface geometry and crystalline structures of aligned TiO_2 nanotubes for photoelectrochemical water splitting. *Sci. Rep.* **8**(1), 10870 (2018). <https://doi.org/10.1038/s41598-018-29247-3>
- Soleymani, S., Ghaderi, A., Dejam, L., Garczyk, Ż., Sapota, W., Stach, S., Dalouji, V., Luna, C., Elahi, S.M., Elahi, S.H.: Correlation between the multifractal structure, crystalline and photoluminescence properties of engineered CZO thin films. *Int. J. Hydrog. Energy* **42**(20), 14205–14219 (2017). <https://doi.org/10.1016/j.ijhydene.2017.04.045>
- Dejam, L., Mohammad Elahi, S., Nazari, H.H., Elahi, H., Soleymani, S., Ghaderi, A.: Structural and optical characterization of ZnO and AZO thin films: the influence of post-annealing. *J. Mater. Sci. Mater. Electron.* **27**(1), 685–696 (2015). <https://doi.org/10.1007/s10854-015-3804-7>
- Dalouji, V., Soleymani, S., Dejam, L., Elahi, S.M., Rezaee, S., Mehrparvar, D.: Gap states of ZnO thin films by new methods: optical spectroscopy, optical conductivity and optical dispersion energy. *Chin. Phys. Lett.* **35**(2), 027701 (2018). <https://doi.org/10.1088/0256-307x/35/2/027701>
- Pal, P.P., Manam, J.: Evaluation of kinetics parameters in the X-irradiated TSL studies of RE^{3+} -doped ($\text{RE} = \text{Eu}, \text{Tb}$) ZnO nanorods for dosimetric applications. *Appl. Phys. A* **116**(1), 213–223 (2013). <https://doi.org/10.1007/s00339-013-8095-3>
- Geetha Devi, P., Sakthi Velu, A.: Synthesis, structural and optical properties of pure ZnO and Co doped ZnO nanoparticles prepared by the co-precipitation method. *J. Theor. Appl. Phys.* **10**, 233–240 (2016). <https://doi.org/10.1007/s40094-016-0221-0>
- Devi, P.G., Velu, A.S.: Synthesis, structural and optical properties of pure ZnO and Co doped ZnO nanoparticles prepared by the co-precipitation method. *J. Theor. Appl. Phys.* **10**(3), 233–240 (2016). <https://doi.org/10.1007/s40094-016-0221-0>
- Shahroosvand, H., Ghorbani-asl, M.: Solution-based synthetic strategies for Eu doped ZnO nanoparticle with enhanced red photoluminescence. *J. Lumin.* **144**, 223–229 (2013). <https://doi.org/10.1016/j.jlumin.2013.06.003>
- Ökte, A.N.: Characterization and photocatalytic activity of Ln (La, Eu, Gd, Dy and Ho) loaded ZnO nanocatalysts. *Appl. Catal. A Gen.* **475**, 27–39 (2014). <https://doi.org/10.1016/j.apcat.a.2014.01.019>
- Akazawa, H., Shinojima, H.: Relation between process parameters of ZnO host films and optical activation of doped Er^{3+} ions. *Mater. Sci. Eng. B* **178**, 1032–1039 (2014). <https://doi.org/10.1016/j.mseb.2014.07.007>
- Kumar, V., Kumar, V., Som, S., Duvenhage, M.M., Ntwaeaborwa, O.M., Swart, H.C.: Effect of Eu doping on the photoluminescence properties of ZnO nanophosphors for red emission applications. *Appl. Surf. Sci.* **308**, 419–430 (2014). <https://doi.org/10.1016/j.apsusc.2014.04.192>
- Thomas, K., Alexander, D., Sisira, S., Biju, P.R., Unnikrishnan, N.V., Ittyachen, M.A., Joseph, C.: NUV/blue LED excitable intense green emitting terbium doped lanthanum molybdate nanophosphors for white LED applications. *J. Mater. Sci. Mater. Electron.* **28**(23), 17702–17709 (2017). <https://doi.org/10.1007/s10854-017-7708-6>
- Huang, M., Wang, S., Wan, G., Zhang, X., Zhang, Y., Ou, K., Yi, L.: Effect of co-doped Tb^{3+} ions on electroluminescence of

- ZnO:Eu³⁺ LED. *J. Mater. Sci. Mater. Electron.* (2018). <https://doi.org/10.1007/s10854-018-8709-9>
16. Kwon, S.H., Moon, B.K., Choi, B.C., Jeong, J.H., Kim, J.H.: Syntheses and luminescent properties of CaAl₂Si₂O₈:Eu²⁺, Mn²⁺ phosphors for white LED. *J. Korean Phys. Soc.* **68**(2), 363–367 (2016). <https://doi.org/10.3938/jkps.68.363>
 17. Han, L., Sun, Y., Sun, J.: Synthesis and luminescence properties of white-light-emitting phosphor Sr₃GdNa(PO₄)₃F:Dy³⁺. *J. Rare Earth* **34**(1), 12–16 (2016). [https://doi.org/10.1016/s1002-0721\(14\)60571-8](https://doi.org/10.1016/s1002-0721(14)60571-8)
 18. Shahroosvand, H., Ghorbani-asl, M.: Solution-based synthetic strategies for Eu doped ZnO nanoparticle with enhanced red photoluminescence. *J. Lumin.* **144**, 223–229 (2013). <https://doi.org/10.1016/j.jlumin.2013.06.003>
 19. Wang, M., Huang, C., Huang, Z., Guo, W., Huang, J., He, H., Wang, H., Cao, Y., Liu, Q., Liang, J.: Synthesis and photoluminescence of Eu-doped ZnO microrods prepared by hydrothermal method. *Opt. Mater.* **31**(10), 1502–1505 (2009). <https://doi.org/10.1016/j.optmat.2009.02.009>
 20. Che, P., Meng, J., Guo, L.: Oriented growth and luminescence of ZnO:Eu films prepared by sol–gel process. *J. Lumin.* **122–123**, 168–171 (2007). <https://doi.org/10.1016/j.jlumin.2006.01.076>
 21. Rasouli, S., Arabi, A.M., Naeimi, A., Hashemi, S.M.: Microwave-assisted combustion synthesis of ZnO:Eu nanoparticles: effect of fuel types. *J. Fluoresc.* **28**(1), 167–172 (2018). <https://doi.org/10.1007/s10895-017-2179-y>
 22. Cho, S.: Synthesis and luminescent properties of Eu³⁺-doped ZnO phosphors. *J. Korean Phys. Soc.* **66**(10), 1559–1563 (2015). <https://doi.org/10.3938/jkps.66.1559>
 23. Cho, S.: Properties of Eu-doped zinc oxide thin films grown on glass substrates by radio-frequency magnetron sputtering. *Curr. Appl. Phys.* **13**(9), 1954–1959 (2013). <https://doi.org/10.1016/j.cap.2013.08.007>
 24. Najafi, M., Haratizadeh, H.: The effects of Al doping and post-annealing via intrinsic defects on photoluminescence properties of ZnO:Eu nanosheets. *Mater. Sci. Semicond. Process.* **31**, 76–83 (2015). <https://doi.org/10.1016/j.mssp.2014.11.021>
 25. Yang, J., Li, X., Lang, J., Yang, L., Wei, M., Gao, M., Liu, X., Zhai, H., Wang, R., Liu, Y., Cao, J.: Synthesis and optical properties of Eu-doped ZnO nanosheets by hydrothermal method. *Mater. Sci. Semicond. Process.* **14**(3–4), 247–252 (2011). <https://doi.org/10.1016/j.mssp.2011.04.002>
 26. Tsuji, T., Terai, Y., Kamarudin, M.H.B., Yoshida, K., Fujiwara, Y.: Concentration quenching in Eu-doped ZnO grown by sputtering-assisted metalorganic chemical vapor deposition. *J. Lumin.* **132**(12), 3125–3128 (2012). <https://doi.org/10.1016/j.jlumin.2011.12.042>
 27. Pan, C.J., Chen, C.W., Chen, J.Y., Huang, P.J., Chi, G.C., Chang, C.Y., Ren, F., Pearton, S.J.: Optical and structural properties of Eu-diffused and doped ZnO nanowires. *Appl. Surf. Sci.* **256**(1), 187–190 (2009). <https://doi.org/10.1016/j.apsusc.2009.07.108>
 28. Lupan, O., Pauporté, T., Viana, B., Aschehoug, P., Ahmadi, M., Cuenya, B.R., Rudzevich, Y., Lin, Y., Chow, L.: Eu-doped ZnO nanowire arrays grown by electrodeposition. *Appl. Surf. Sci.* **282**, 782–788 (2013). <https://doi.org/10.1016/j.apsusc.2013.06.053>
 29. Ding, M., Chen, D., Yin, S., Ji, Z., Zhong, J., Ni, Y., Lu, C., Xu, Z.: Simultaneous morphology manipulation and upconversion luminescence enhancement of β-NaYF₄:Yb³⁺/Er³⁺ microcrystals by simply tuning the KF dosage. *Sci. Rep.* **S12745**, 1–14 (2015). <https://doi.org/10.1038/srep12745>
 30. Assadi, M.H.N., Zhang, Y., Zheng, R.: Structural and electronic properties of Eu- and Pd-doped ZnO. *Nanoscale Res. Lett.* **6**, 357 (2011)
 31. Geburt, S., Lorke, M., da Rosa, A.L., Frauenheim, T., Roder, R., Voss, T., Kaiser, U., Heimbrodt, W., Ronning, C.: Intense intrashell luminescence of Eu-doped single ZnO nanowires at room temperature by implantation created Eu–O_i complexes. *Nano Lett.* **14**(8), 4523–4528 (2014). <https://doi.org/10.1021/nl5015553>
 32. Flemban, T.H., Sequeira, M.C., Zhang, Z., Venkatesh, S., Alves, E., Lorenz, K., Roqan, I.S.: Identifying the influence of the intrinsic defects in Gd-doped ZnO thin-films. *J. Appl. Phys.* **119**(6), 065301 (2016). <https://doi.org/10.1063/1.4941434>
 33. Tingqiao, L.E.O.W., Li, H., Hussin, R., Ibrahim, Z., Deraman, K., Lintang, H.O., Shamsuri, W.N.W.: Effects of Eu³⁺ and Dy³⁺ doping or co-doping on optical and structural properties of BaB₂Si₂O₈ phosphor for white LED applications. *J. Rare Earths* **34**, 21–29 (2016)

Publisher's Note Springer Nature remains neutral with regard to jurisdictional claims in published maps and institutional affiliations.